International Journal of Applied Power Engineering (IJAPE)
Vol. 4, No. 1, April 2015, pp. 13~22
ISSN: 2252-8792

Comparison between Two-Level Converter and Three-Level NPC Converter for Evaluation the Quality Power of DFIG Based Wind Turbines

Zerzouri Nora*, Labar Hocine*, Kechida Sihem**
* Department of Electrical Engineering, Badji Mokthar University Annaba, Algeria
** Automatic Control Laboratory and Computer Guelma Laig, University of Guelma, BP 401.Guelma 24000, Algeria

Article Info

Article history:

Received Jun 26, 2015
Revised Feb 10, 2015
Accepted Mar 23, 2015

Keyword:

DoublyFed Induction Generator
PWM Technique
Total Harmonics
Wind Turbine

ABSTRACT

This paper deals the power control for three-level voltage source inverter NPC-VSI feeds the rotor of the doubly fed induction generator 'DFIG' based wind power generation system. This converter allows controlling the rotor voltage in magnitude and phase angle with a high flexibility and can therefore be used for active and reactive power control of DFIG. The control is especially designed to reduce the harmonic distortion of the generated currents and active power ripples of the classical control. In addition, it's convenient for high power drive and variable speed generator applications with constant switching frequency. The detailed operation principle and simulation results for 3 MW of DFIG are also discussed.

Corresponding Author:

Zerzouri Nora,
Departement of Electrical Engineering,
Badji Mokthar University Annaba,
Université Badji Mokhtar -Annaba- B.P.12, Annaba, 23000 Algeria.
Email: nzerzouri@yahoo.fr

1. INTRODUCTION

With the fast increasing of wind energy installed capacity over the last two decades, it is playing a vital role in world's energy markets at the present. It is expected that global total wind power generation will supply around 12% of the total world electricity generation at the end of 2020. Currently the preferred configuration for wind turbine generation is doubly fed induction generator, which can be seen in Fig. 1. This can be due to their advantageous characteristics. In comparison with the fixed speed wind turbine, they can reduce mechanical stresses, and compensate for torque and power pulsations, and as a result improve power quality. In addition, variable speed turbines can maximize the efficiency of the energy conversion, as they can operate at optimal rotational velocity for each given wind speed [1]. The DFIG with a vector control strategy delivers good performance and is commonly used in wind turbine industry [2]. There are many reasons for using a DFIG for a variable wind speed, such as reducing strain on mechanical parts, noise and the possibility for control active and reactive power [3]. The wind system using a DFIG and the back-to-back Pulse Width Modulation (PWM) converter which connects the rotor of the generator and the network has many advantages. One of them is the power converters used that are sized to pass a fraction of the total power of the system [4]-[5], there by reducing losses in power electronic components. The performance and output power do not depend only on the DFIG, but also the way the back-to-back converter is controlled. The back-to-back converter consists of two parts: the machine side converter called Rotor Side Converter (RSC) and the network side converter called Grid Side Converter (GSC). The RSC controls the active power and reactive power produced by the machine. The GSC controls the DC bus voltage and power factor. In this

study, a technique to control the two and three level inverter is presented and the wind system dynamic performance is analyzed by simulations in Matlab / Simulink. Firstly, the wind turbine is modelled then a MPPT technique for extracting the maximum power is presented. Subsequently, a model of the DFIG is derived in dq reference frame and presented the model of two and three level inverter. Finally, simulation results and their interpretation are provided.

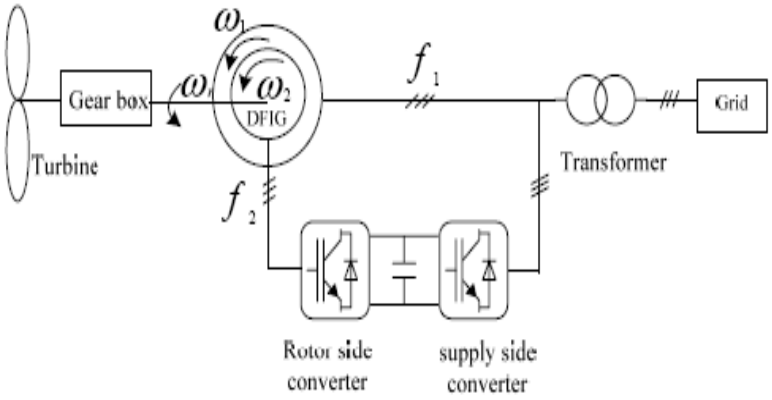

Figure 1. Wind turbine system with doubly fed induction generator

2. MODEL OF THE WIND TURBINE AERODYNAMICS

The mechanical power extracted from a wind turbine, P_T, is dependent on the power coefficient, C_p, for the given turbine operation conditions and is given by

$$P_t = \frac{1}{2}\rho A C_p(\lambda,\beta)v^3 \quad (1)$$

Where C_p, A, ρand v are the power coefficient (maximum value Betz's limit 0.593), the area swept by the blades, the specific density of air and the wind speed, respectively. Therefore, if the air density, swept area and wind speed are constant, the output power of the wind turbine will be a function of C_p. However, C_p is a function of the pitch angel of turbine rotor blades, β, and the tip-speed ratio, $\boldsymbol{\lambda}$, which is defined as

$$\lambda = \frac{\Omega R}{v} \quad (2)$$

Where Ω is the speed of turbine and R the blade radius.
The power coefficient of the turbine is given by [6]:

$$C_p(\lambda,\beta) = c_1\left(c_2\frac{1}{A} - c_3\beta - c_4\right)e^{-c_5\frac{1}{A}} + c_6\lambda \quad (3)$$

A typical C_p curve is shown in Figure 2.

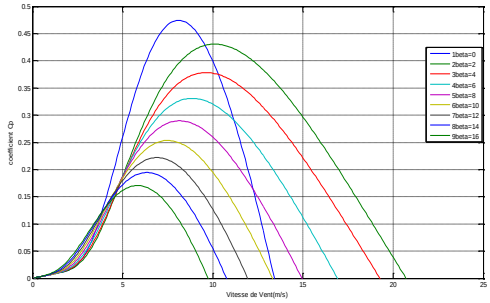

Figure 2. Power coefficient *C p* versus tip speed ratio $\boldsymbol{\lambda}$

The parameters of wind turbine for this calculation are shown in Table IV. The same parameters are also adopted in simulation of section V. As it can be seen, there is a value of λ for which C_p value is maximized (C_{pmax}) by a given pitch angle β value, and the C_{pmax} value is reduced with the β value increased. To extract the maximum wind energy, pitch angle is usually around zero when the winds speed below the rated value [7].

With constant blade pitch angle, the maximum value of the power coefficient C_{pmax} would be obtained at a particular value of $\boldsymbol{\lambda}$, defined as $\boldsymbol{\lambda}_{opt.}$ For maximum power point tracking (MPPT), $\boldsymbol{\lambda}$ should be maintained at this optimal value. The Maximum output power of the wind turbines P_{tmax} can be expressed by [7],[8]:

$$P_{tmax} = \frac{1}{2}\rho A C_{pmax} v^3 \tag{4}$$

3. DFIG MODELLING AND POWER CONTROL

3.1. Doubly Fed Induction Machine Equations

The DFIG is a wound rotor induction generator in which the rotor circuit is connected to the grid through two back-toback converters and a dc-link capacitor [9]. The ability to subtract and supply power from the rotor makes it possible to operate the DFIG at subsynchronous or supersynchronous speed while keeping constant the voltage and frequency on the stator. The $d-q$ model in an arbitrary reference frame is expressed as follows [10], [11]:

$$\begin{cases} V_{ds} = R_s I_{ds} + \frac{d\phi_{ds}}{dt} - \phi_{qs}\omega_s \\ V_{qs} = R_s I_{qs} + \frac{d\phi_{qs}}{dt} + \phi_{ds}\omega_s \\ V_{dr} = R_r I_{dr} + \frac{d\phi_{dr}}{dt} - \phi_{qr}(\omega_s - \omega_r) \\ V_{qr} = R_r I_{qr} + \frac{d\phi_{qr}}{dt} + \phi_{dr}(\omega_s - \omega_r) \end{cases} \tag{5}$$

The flux equations are:

$$\begin{cases} \phi_{ds} = L_s I_{ds} + M I_{dr} \\ \phi_{qs} = L_s I_{qs} + M I_{qr} \\ \phi_{dr} = L_r I_{dr} + M I_{ds} \\ \phi_{qr} = L_r I_{qr} + M I_{qs} \end{cases} \tag{6}$$

Where
ω_s: synchronous angular frequency
ω_r: rotor angular frequency
Rs, *Rr*: equivalent resistances of stator and rotor windings, respectively
Ls, *Lr*, *M*: self and mutual inductances of stator and rotor windings, respectively
The motion equations are given as follows:

$$\frac{d\omega_r}{dt} = \frac{C_m - C_e}{J} \tag{7}$$

$$C_e = \frac{3}{2} PM(I_{qs} I_{dr} - I_{ds} I_{qr}) \tag{8}$$

$$\omega_g = s\omega_s = \omega_s - \omega_r \tag{9}$$

Where
ω_g: slip angular frequency
s: slip
C_m: mechanical torque provided to the wind turbine
C_e: electromagnetic torque
J: moment of inertia

3.2. Rotor side Converter

In the rotor side converter, reactive power and the referenced torque determine the current references, which determine the voltages to be applied to the rotor side.

A wind-turbine generator must be fully controllable so that it can operate at a shaft speed that is independent of wind conditions to gain the stator voltage which is the same to grid voltage, including the same amplitude, frequency and phase.

In this section, the control model of rotor side converter is analyzed. The stator flux orientation refers to the d-axis synchronous rotating dq coordinate system oriented in the direction of the doubly-fed motor stator flux, shown in Figure 3.

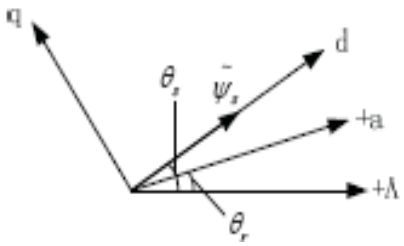

Figure 3. Stator field oriented control of DFIG

We can obtain the following relationship:

$$\begin{cases} \phi_{ds} = \phi_s \\ \phi_{qs} = 0 \end{cases} \tag{10}$$

To keep the stator flux ϕ_s constant, the voltage equations can be expressed as:

$$\begin{cases} V_{ds} \approx \frac{d\phi_{ds}}{dt} = 0 \\ V_{ds} \approx \frac{d\phi_{ds}}{dt} = V_s \end{cases} \tag{11}$$

Where V_s is the space vector amplitude of stator voltage.

The active and reactive powers of stator can be derived as:

$$\begin{cases} P_s = \frac{3}{2}(V_{ds}I_{ds} + V_{qs}I_{qs}) \approx \frac{3}{2}V_sI_{qs} \\ Q_s = \frac{3}{2}(V_{qs}I_{ds} - V_{ds}I_{qs}) \approx \frac{3}{2}V_sI_{ds} \end{cases} \tag{12}$$

From above power equations, it is clear to describe the power flow in the DFIG for sub-synchronous and supersynchronous operation. Above synchronous speed, the fourquadrant converter operates as a generator of active power delivering power to the grid .Under the condition of subsynchronous; the four-quadrant converter circulates active power from the grid into the rotor circuit.

Using equations (10) to (6), the rotor currents can be derived in the following form.

$$\begin{cases} I_{ds} = \frac{MI_{dr} - \phi_{ds}}{L_s} \\ I_{qs} = \frac{M}{L_s}I_{qr} \end{cases} \tag{13}$$

Finally, the rotor reference voltages are calculated using

$$\begin{cases} V_{dr} = R_rI_{dr} + \delta L_r\frac{dI_{dr}}{dt} - \omega_g\delta L_rI_{qr} \\ V_{qr} = R_rI_{qr} + \delta L_r\frac{dI_{qr}}{dt} + \omega_g\delta L_rI_{dr} + \frac{M}{L_s}\phi_{ds} \end{cases} \tag{14}$$

It is clear from the stator power expressions (10), that stator active power is controlled by I_{dr}, while I_{qr} controls stator reactive power.

The RSC control strategy is illustrated in Figure 4. For the stator to operate at unity power factor, the flow of reactive power from the stator side to grid is set to zero, thus I_{rq}*can be determined from (10), so I_{dr}* can be calculated from (12). Now the actual rotor currents I_{dr} and I_{qr} are compared with the reference rotor currents I_{dr} * and I_{qr} * before being processed using inner PI current controllers, in a similar manner to the ones used for GSC, then added with cross-terms, to finally generate the control signals for the RSC[10].

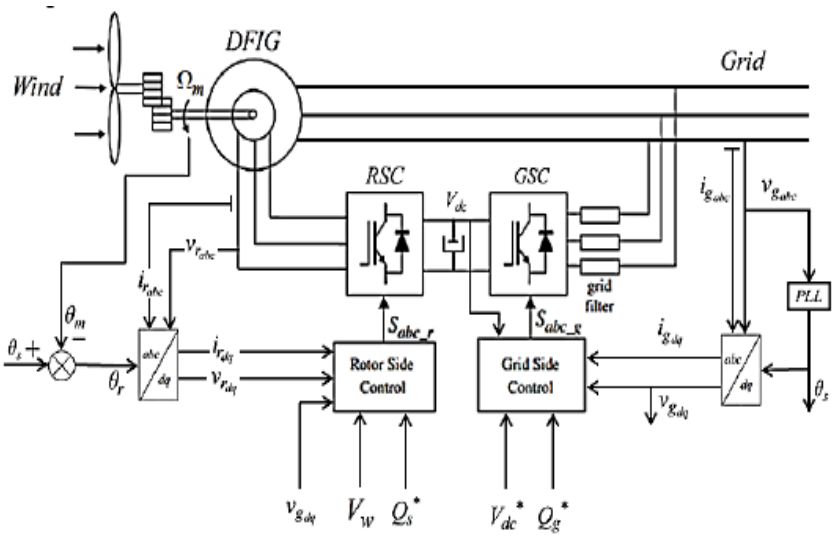

Figure 3. Vector control of DFIG with grid and rotor side converters.

4. MODELLING PWM INVERTER

4.1. Two-level inverters

A power circuit of three-phase voltage-source back-to back PWM converters including two lelve power semiconductor switches is shown in Figure 5, where the two converters are linked through a DC capacitor. As can be seen in Figure5, the DC/AC inverter has an input voltage (Vdc) and produces three output voltage(va'(t); vb'(t); vc'(t)) , which is the input voltage of the inverter, whereas the three phase voltages (va(t); vb(t); vc(t)) designate the input terminal of the converter

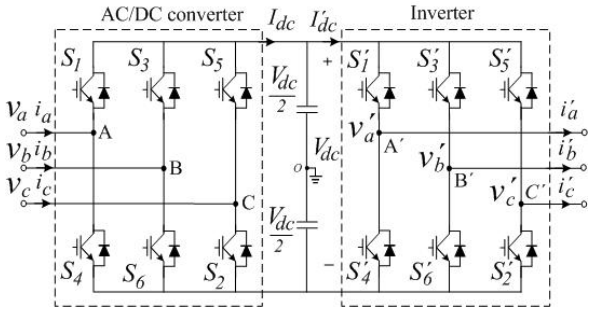

Figure 5. Circuit configuration of two-level back-to-back PWM converters.

The PWM technique is obtained by comparison of a triangular carrier waveform with the reference sinusoidal waveform at the fundamental frequency of the output voltage. Then, the switching pulses (S_1'; S_4') for phase A are illustrated in Table 1

Table 1. Switching states of Two-Level One-Phase Inverter

Switching states		Output voltage (v_{ao})
S_1'	S_4'	
1	0	*Vdc/2*
0	1	*-Vdc/2*

4.2. Inverter Model

The output voltages (v_{ab}' (t),v_{bc}'(t),v_{ca}'(t)) are made up by using switching functions. Where can be formulated as followings:

$$\begin{cases} v'_{ab}(t) = S'_a(t)V_{dc} \\ v'_{bc}(t) = S'_b(t)V_{dc} \\ v'_{ca}(t) = S'_c(t)V_{dc} \end{cases} \quad (15)$$

Where Sa'(t), Sb'(t), and Sc'(t) are switching functions for each leg of a two-level DC/AC inverter. The function model for a DC/AC inverter can be expressed as:

$$\begin{cases} S'_a(t) = \frac{1}{2}(S'_1 - S'_4) \\ S'_b(t) = \frac{1}{2}(S'_3 - S'_6) \\ S'_c(t) = \frac{1}{2}(S'_5 - S'_2) \end{cases} \quad (16)$$

4.3. Three Level Inverter

The circuit configuration of three-level back-to back PWM converters consists of two neutral-point clamped converters, linked through DC capacitors, which is shown in Figure5. Each inverter uses twelve switches and six additional diodes.

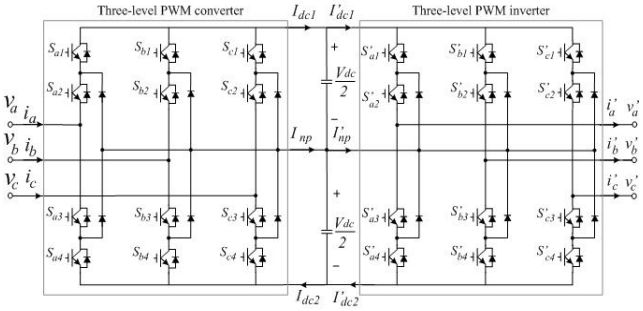

Figure 5. Circuit configuration of three-level back-to-back PWM converters.

To generate the switching pulses for the inverters, two carrier waveforms are simultaneously compared with a sinusoidal waveform at the fundamental frequency. In the case of phase A, for instances, the switching pulses (Sa1; Sa2; Sa3; Sa4) are described in Table 2.

Table 2. Switching states of Three-Level One-Phase Inverter

Switching states					Output voltage (v_{ao})
Sa1'	Sa2'	Sa3'	Sa4'	Sa'	
1	1	0	0	+	*+Vdc/2*
0	1	1	0	0	0
0	0	1	1	-	*-Vdc/2*

4.4. Inverter Model

The output voltages (v_a' (t),v_b'(t),v_c'(t)) are made up by using switching functions. Where can be formulated as followings:

$$\begin{cases} v'_a(t) = S'_a(t)V_{dc} \\ v'_b(t) = S'_b(t)V_{dc} \\ v'_c(t) = S'_c(t)V_{dc} \end{cases} \quad (17)$$

Where Sa'(t), Sb'(t), and Sc'(t) are switching functions for each leg of a three-level DC/AC inverter. The function model for a DC/AC inverter can be expressed as:

$$\begin{cases} S'_a(t) = \frac{1}{2}(S'_{a1}S'_{a2} - S'_{a4}S'_{a3}) \\ S'_b(t) = \frac{1}{2}(S'_{b1}S'_{b2} - S'_{b4}S'_{b3}) \\ S'_c(t) = \frac{1}{2}(S'_{c1}S'_{c2} - S'_{c4}S'_{c3}) \end{cases} \quad (18)$$

5. SIMULATION RESULTS

Simulation results were performed using software Matlab / Simulink. To validate the controls proposed in this paper, we present two operating points in hypo-or hyper-synchronous fashion. For these simulations, we consider that the wind system is steady and working in the zone of optimal functioning (zone 2), that is to say that it produces maximum power versus speed of the wind. The reference voltage of the DC link is set at 1200V. We have vary the stator reactive power Qs playing on its reference value. The parameters of the DFIG are given in Table III.

5.1. Wind power system operation mode hypo synchronous.

For this mode, a wind velocity equal to 8ms^{-1} is applied on wind turbine blades, which corresponds to a speed of DFIG in MPPT control approximately 1380 tr/min, a shift 30% hypo synchronous mode, as shown in Figure 7.

Figure 8 shows the temporal evolution of the various power supply Qs, Ps and Pr, Qr. At time t = 2s, the wind system operates as a unity power factor and reactive power Qs_ref imposed zero. From time t = 2s to t = 3,5s, we set the stator reactive power reference equal to -1MVar corresponding to changes in the reference direct current rotor and also on the rotor reactive power Qr. From time t = 3.5s we set the stator reference reactive power equal to 1 MVar, again, different reactive powers are properly regulated.

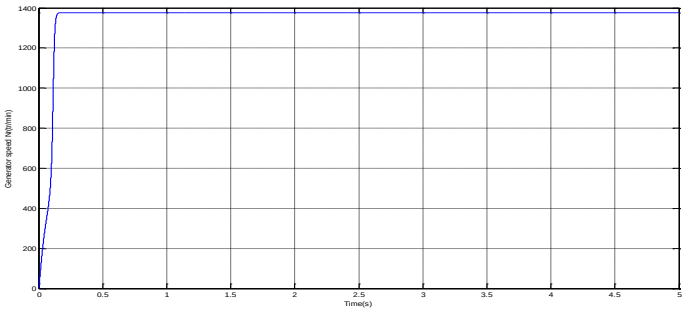

Figure 7.Generator speed

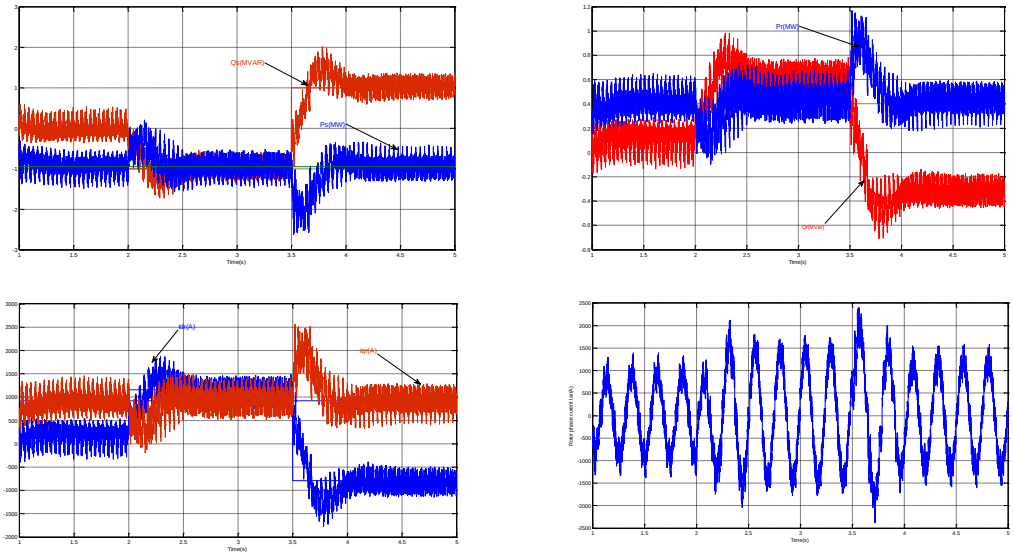

Figure 8. Ps, Qs, Pr, Qr, ird, irq and iar (hyposynchronous)

5.2. Wind power system operation mode hyper synchronous

For this mode, a wind speed equal to 11m/s corresponds to the nominal operation of the turbine is applied on wind turbine blades, which corresponds to a speed of DFIG in MPPT control approximately 1950 tr /min, a shift of -30% hyper synchronous mode, as shown in Figure 9 and Figure 10. The same stator reactive power variations have been applied to this mode as the previous. We also note that the d q axis rotor currents are perfectly decoupled through the decoupling strategy by ensuring natural PWM. We also observe the rotor phase current follows perfectly the reference obtained by the orientation of the stator flux. Both modes are validated and independent control of different powers of the wind system.

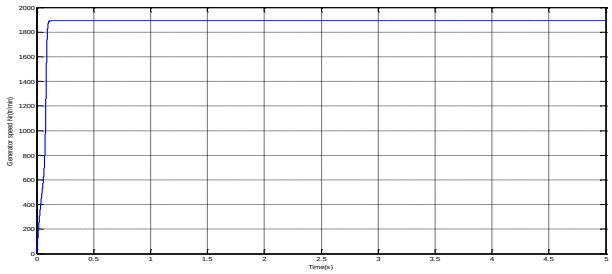

Figure 9.Generator speed

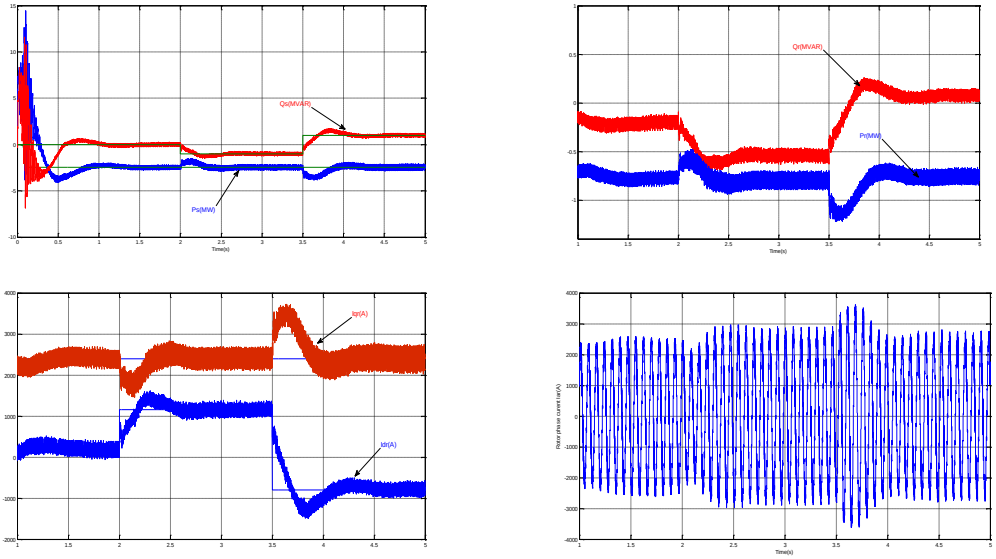

Figure 10.Ps, Qs, Pr, Qr, ird, irq and iar (hypersynchronous)

Figure 11 and Figure 12 show the harmonic spectrum of output phase stator current obtained using Fast Fourier Transform (FFT) technique for PWM for 2-level and 3-level inverter respectively. It can be clear observed that all the lower order harmonics are reduced for 3-level inverter (THD = 3.88%) when compared to 2-level inverter (THD = 4.09%).

(a) (b)

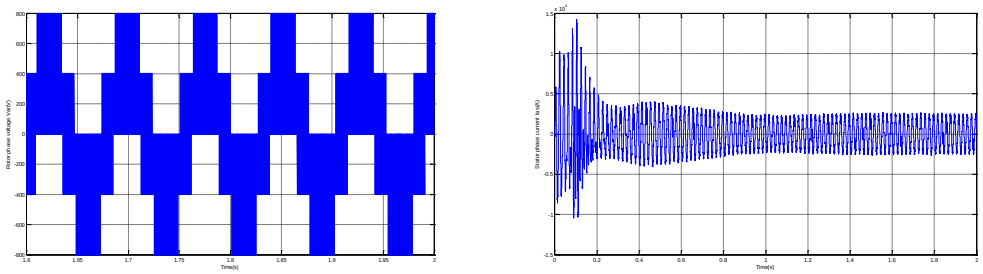

(c)

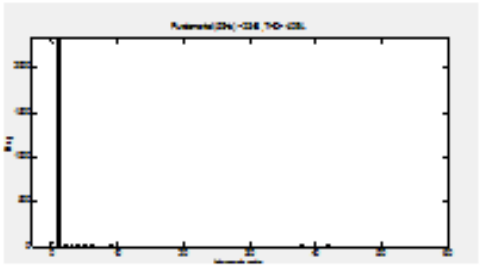

Figure 11. (a) Rotor phase voltage, (b) Stator phase current, (c) Spectrum harmonics using 2-level

(a) (b)

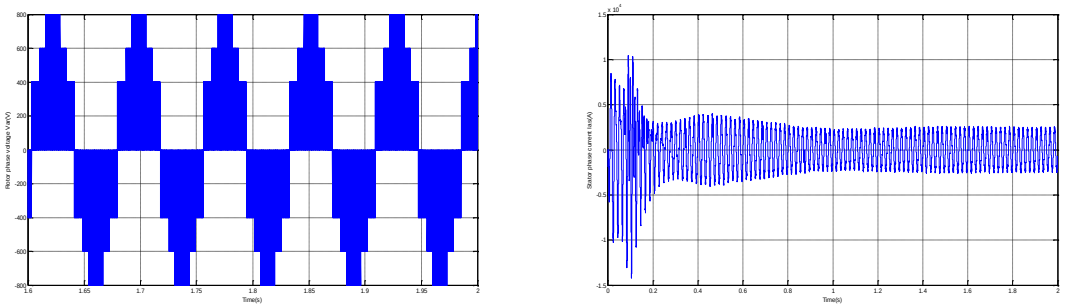

(c)

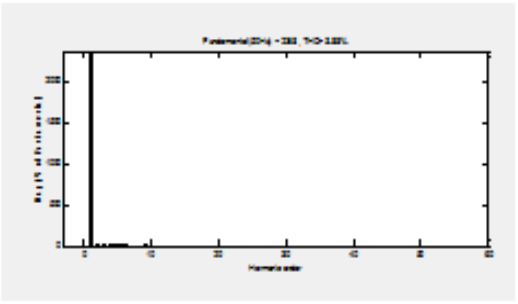

Figure 12. (a) Rotor phase voltage, (b) Stator phase current, (c) Spectrum harmonics using 3-level

Table 3. 3MW WTG Induction Machine Parameters

parametre	value
Rotor resistor per phase	2,97mΩ
Rotor resistor per phase	3,82mΩ
Inductance of the stator winding	121 mH
Inductance of the retor winding	57,3 mH
Mutual Inductance	12,12 mH
Number of pole pairs	2
Inertia	114 kg.m2
Rated power	3MW
Rated voltage	690V

Table 4.The parameters of wind turbine

parametre	value
Nomber of blade	3
Reted speed	11m/s
Inertia	114 kg.m^2
Gearbox ratio	100
Rotor Diameter	45m

6. CONCLUSION

This paper presents simulation results of Field orientation method control for active and reactive power control of a DFIG, using the modulation strategy of the PWM inverter for two and three level. With results obtained from simulation, it is clear that for the same operation condition, the DFIG active and reactive power control with field oriented control using in the three level had better performance than the PWM technique two level and that is clear in the spectrum of phase stator current harmonics which the use of the three level, it is reduced of harmonics more than two level inverter.

REFERENCES

[1] A. Babaie Lajimi, S. Asghar Gholamian, M. Shahabi. Modeling and Control of a DFIG-Based Wind Turbine during a Grid Voltage Drop. ETASR - Engineering, Technology & Applied Science Research Vol. 1, No. 5, 2011, 121-125.

[2] M A. Mossa .Field Orientation Control of a Wind Driven DFIG Connected to the Grid. WSEAS TRANSACTIONS on POWER SYSTEMS, Issue 4, Volume 7, October 2012.

[3] A.Boumassata, D.Kerdoun, N.Cherfia, N.Bennecib. Performance of wind energy conversion systems using a cycloconverter to control a doubly fed induction generator. Energy Procedia 42 (2013) 143 – 152 [Mediterranean Green Energy Forum MGEF13].

[4] Sai Sindhura K, G. Srinivas Rao**.** Control and Modeling of Doubly Fed Induction Machine for Wind Turbines. Int. Journal of Engineering Research and Applications, Vol. 3, Issue 6, Nov-Dec 2013, pp.532-538.

[5] Srinath Vanukuru, Sateesh Sukhavasi**.** Active & Reactive Power Control Of A Doubly Fed Induction Generator Driven By A Wind Turbine. International Journal of Power System Operation and Energy Management, ISSN (PRINT): 2231–4407, Volume-1, Issue-2, 2011.

[6] Zhen Sun, Hongyu Wang, Ying Li. *Modelling and Simulation of Doubly-Fed Induction Wind Power System Based on Matlab/Simulink*. Sustainable Power Generation and supply (Supergen 2012), Intrnational Conference on,8-9sept.2012,page(s). 1-5.

[7] H. Li., Z. Chen. *Optimal Power Control Strateay of Maximizina Wind Eneray Trackina and Conversion for VSCF Doubly Fed Induction Generator System*. Power Electronics and Motion Control Conference, 2006. IPEMC 2006. CES/IEEE 5th International, Volume 3, Publication Year: 2006, Page(s): 1 - 6, IEEE CONFERENCE PUBLICATIONS.

[8] J. Tian. *Reactive Power Capability of the Wind Turbine with Doubly Fed Induction Generator*. Industrial Electronics society IECON 2013, 39th Annual Conference of the IEEE, Publication Year: 2013, Page(s): 5312 – 5317.

[9] Dongkyoung Chwa, Kyo-Beum Lee .Variable Structure Control of the Active and Reactive Powers for a DFIG in Wind Turbines. *IEEE* TRANSACTIONS ON INDUSTRY APPLICATIONS, VOL. 46, NO. 6, NOVEMBER/DECEMBER 2010.

[10] Mohammad Sleiman, Bachir Kedjar, Abdelhamid Hamadi, Kamal Al-Haddad, Hadi Y. Kanaan. *Modelina, Control and Simulation of DFIG for Maximum Power Point Tracking*. Control Conference (ASCC), 2013 9th Asian, Publication Year: 2013, Page(s): 1 – 6, IEEE CONFERENCE PUBLICATIONS.

[11] Zerzouri Nora, Labar Hocine .Active and Reactive Power Control of a Doubly Fed Induction Generator. International Journal of Power Electronics and Drive System (IJPEDS).Vol. 5, No. 2, October 2014, pp. 244~251.